Evolution of a shoaling internal solitary wavetrain

D. Bourgault,[1] M. D. Blokhina,[1] R. Mirshak,[2] and D. E. Kelley[2]

Received 12 October 2006; revised 14 December 2006; accepted 29 December 2006; published 2 February 2007.

[1] Field observations of an internal solitary wavetrain impacting a shoaling bottom are presented. Measurements of the spatio-temporal characteristics of the shoaling waves are given, as well as estimations of the mixing they may have caused upon impact. The observations are discussed in the context of numerical simulations, laboratory experiments, and hypotheses recently raised on the origin and evolution of internal solitary waves in coastal environments. **Citation:** Bourgault, D., M. D. Blokhina, R. Mirshak, and D. E. Kelley (2007), Evolution of a shoaling internal solitary wavetrain, *Geophys. Res. Lett.*, *34*, L03601, doi:10.1029/2006GL028462.

1. Introduction

[2] Internal solitary waves (ISWs) are increasingly regarded as an integral component of coastal oceans, especially with respect to their suspected role as vertical mixing agents [*Helfrich and Melville*, 2006]. Despite four decades of research on ISWs, it is not yet clear how to predict the location, timing and magnitude of the mixing they may cause. A particular challenge in developing a parameterization scheme for ISWs mixing is to permit a nonlocal view, in which waves generated at one location cause mixing when they encounter destabilizing conditions elsewhere.

[3] In this paper, we focus on the evolution of an internal solitary wavetrain upon impact with a natural shoaling bottom. Field observations and with the result of a numerical simulation are discussed in the context of the laboratory experiments of *Michallet and Ivey* [1999] and *Helfrich* [1992] and the field observations of *Klymak and Moum* [2003] and *Scotti and Pineda* [2004].

2. Methods

[4] Building upon the work of *Bourgault and Kelley* [2003] and *Bourgault et al.* [2005], a field experiment took place on the flank of Ile-aux-Lièvres Island in the St. Lawrence Estuary on 26 August 2004 (Figure 1). Internal wave structure was obtained using a towed Biosonics 200 kHz narrow-beam echosounder. Internal waves detected on the echosounder were associated with visible bands on the sea surface, and the latter were used to maintain a steaming direction orthogonal to the wave propagation direction. Horizontal position was determined to within 5 m with a Global Positioning System unit.

[5] A coordinate system was defined relative to the wave propagation direction (see Figure 1). The position associated with each echosounding measurement was then adjusted for the Doppler shift by remapping the recorded positions x' of every ping with $x = x' - c(t - t')$, where t is time, t' is the time when the wave trough/crest was observed and c is the wave phase velocity determined by the distance the wave trough/crest propagated between two consecutive transects. Visual inspection of the scattering layers on the Doppler-adjusted echogram yielded $\eta(x)$, the wave interfacial displacement relative to the background level. The amplitude was computed as $a = \max(|\eta|)$ and the horizontal lengthscale as $L = (1/a)\int_{x_1}^{x_2} |\eta|\, dx$, where $[x_1, x_2]$ was chosen to include the entire wave.

[6] Two 600 kHz and one 1200 kHz upward-looking RD Instruments broadband acoustic Doppler current profilers (ADCPs) were moored on the slope (Moorings A, B, and C on Figure 1). These instruments recorded the backscatter intensity and the three-dimensional currents in the water column and were set to record 7 s, 15 s, and 10 s ensemble averages with 1.00 m, 0.75 m, and 0.40 m vertical bin sizes, respectively. Mooring C also recorded the near-bottom temperature.

[7] Stratification was inferred from a moored vertical chain (Figure 1). Eleven Minilog −8 bit Vemco thermistors were spaced 2 m apart and recorded temperature every 150 s. In addition, two fast-response conductivity-temperature (CT) recorders (SBE-37, by Sea-Bird Electronics, Inc) were clamped next to the thermistors at depths of 6 m and 18 m, respectively (i.e. above and below the pycnocline, expected to be around 10 m depth) and were set to sample every 15 s. The response time of the thermistors was of the same order as the wave period, $\mathcal{O}$ (100 s), so their sole use was in establishing the background temperature stratification. The CT recorders indicated a tight linear relationship between temperature and salinity (correlation coefficient $R = 0.95$), allowing us to infer density from the thermistor chain.

[8] To help interpret the field observations and to provide qualitative insights into the spatial structure that we did not measure, we set up the two-dimensional non-hydrostatic model of *Bourgault and Kelley* [2003] to simulate an ISW impacting the slope region. The model implementation (topography, grid size, density structure, initial condition) is as by *Bourgault et al.* [2005] except that the density and the incoming ISW amplitude match the present observations.

3. Observations

[9] Figure 2 shows a sequence of echograms that captured the evolution of an ISW of depression shoaling over a bottom of quasi-uniform slope $s = 0.05$, as well as the results of the numerical simulation. The background conditions in which this wave evolved were characterized by

[1]Department of Physics and Physical Oceanography, Memorial University of Newfoundland, St. John's, Newfoundland, Canada.
[2]Department of Oceanography, Dalhousie University, Halifax, Nova Scotia, Canada.

0094-8276/07/2006GL028462$05.00

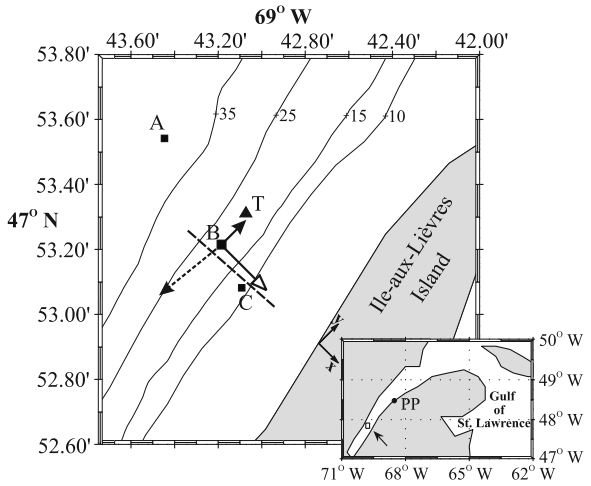

Figure 1. Chart of the field site. The dashed line shows the average transect along which towed measurements were collected. The axis system is indicated with its origin at the island edge. The squares mark Moorings A, B and C and the triangle marks the thermistor and CT chain. The mean surface current is indicated with the solid vector, while the dashed vector represents the mean at 13 m depth, below the pycnocline. The open arrowhead vector indicates the phase speed (c = 0.6 m s^{-1}) and direction of the leading wave of the wavetrain (i.e. the wave on the first panel of Figure 2).

the density structure and currents shown on Figure 3. As it entered the slope region (t = 0), the observed wave had amplitude a = 6.5 m and length L = 64 m. This situation is characterized by Iribarren number $\xi = s/(a/L)^{1/2}$ = 0.16 [*Boegman et al.*, 2005] and is within the range of parameters examined experimentally by *Helfrich* [1992] for ISW breaking and run-up on uniform slopes.

[10] As the wave propagated up-slope its rear steepened, reaching 50° below horizontal at t = 381 s. By t = 488 s the wave had changed into a wave of elevation. In a terminology used by *Helfrich* [1992] and more recently by *Venayagamoorthy and Fringer* [2006, 2007], we will refer to this feature as a "bolus", keeping in mind that other authors have used the term "wave of elevation" to describe similar features. This transition from a wave of depression to a bolus occured without recorded evidence of wave breaking or overturning. However, the shadowgraphs of *Helfrich* [1992] for similar shoaling ISWs (see Helfrich's Figures 3 and 4 for cases corresponding to ξ = 0.38 and ξ = 0.24, respectively) show that overturning and mixing occur on the rear face of the incident ISW and behind the first bolus produced during shoaling. *Boegman et al.* [2005] also report similar observations (their Figures 9g–9l). This process is also seen in the numerical simulation (Figure 2 for $t \geq$ 480 s). These laboratory observations and numerical results suggest that overturning likely occured in the field but was not recorded due to our sampling strategy.

[11] As it continued to move inshore ($t \geq$ 488 s), the bolus remained asymetrical, its front being steeper than its

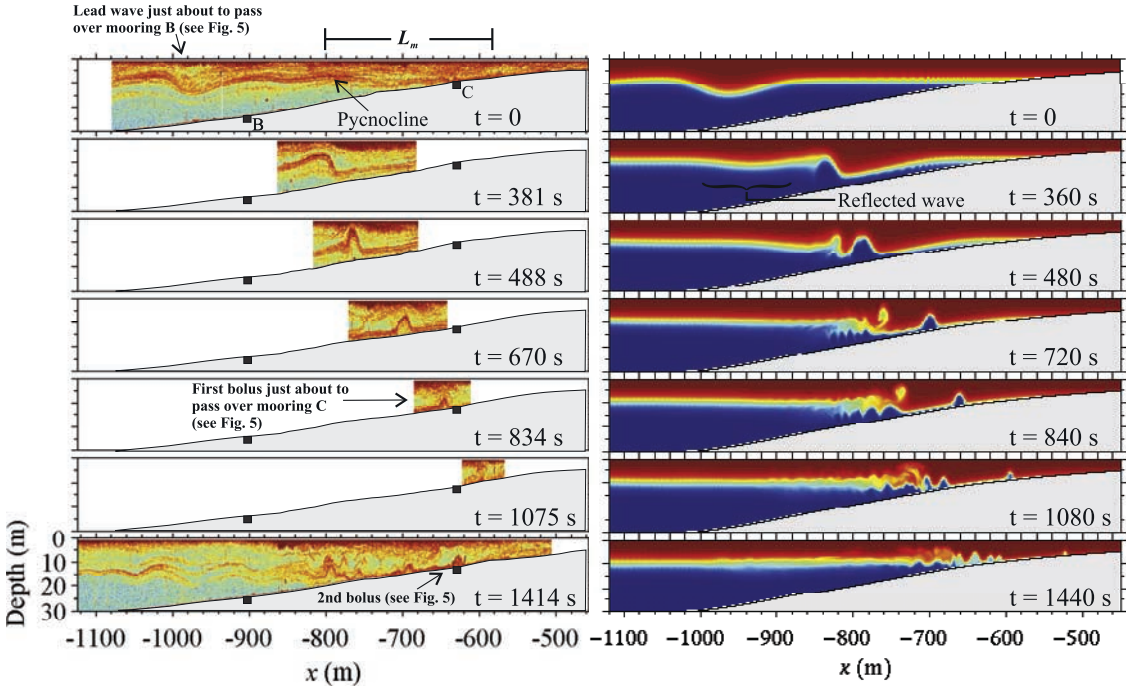

Figure 2. (left) Echograms showing the lead wave (top 6 panels) and the full train (bottom panel) impacting the flank of Ile-aux-Lièvres Island. For conciseness, only 7 transects are shown out of 30 collected. The time corresponds to when the wave trough or crests were sampled, except for the bottom panel where it is the median time of the transect. The origin t = 0 corresponds to 1436 UTC on 26 August 2004. The depth of the pycnocline and of the maximum vertical shear correspond to the high intensity scattering layer observed at 9 m on the top left panel. (right) Results of a numerical simulation showing changes in the density field induced by the shoaling of an ISW with similar characteristics as the observed ISW.

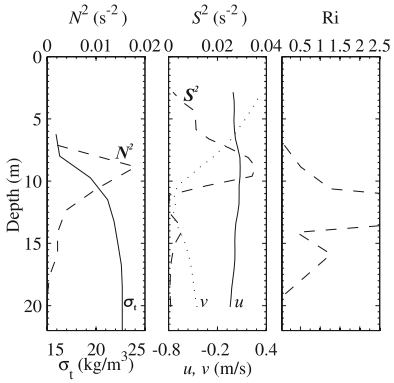

Figure 3. Mean density anomaly σ_t, buoyancy frequency squared $N^2 = -(g/\rho)\ \partial\rho/\partial z$ (where g is the gravitational acceleration and ρ the water density), horizontal currents u (southeastward) and v (northeastward), shear squared $S^2 = (\partial u/\partial z)^2 + (\partial v/\partial z)^2$ and gradient Richardson number $\mathrm{Ri} = N^2/S^2$. The density measurements are from the thermistor-CT chain (triangle on Figure 1) and the current measurements are from Mooring B. Note that the gradient Richardson number near the pycnocline was $1/4 < \mathrm{Ri}|_{z=-9\mathrm{m}} < 1$. These are 5 min averages observed 10 min before the passage of the wavetrain.

rear, as both its amplitude and horizontal lengthscale decreased. The bolus had almost completely dissipated by the pass at $t = 1075$ s, having travelled a distance $L_m = 230 \pm 10$ *m* from its site of formation. Along the bolus path, there is no recorded evidence of overturning or shear instabilities, as also suggested by the numerical simulation.

[12] The bottom panel of Figure 2 shows a slope-wide echogram collected after the leading bolus had dissipated. It reveals that we had sampled the leading wave of a shoaling wavetrain. This echogram shows the spatial structure of the shoaling waves as they approached the slope ($x < -900$ m), changed to boluses ($-800 < x < -750$ m), and then gradually dissipated further up-slope ($x > -750$ m).

[13] Figure 4 shows the up-slope variability of the observed phase speed c, amplitude a, and length L of the lead wave of depression and bolus. The properties remained almost constant prior to the polarity change ($x < -850$ m) but decreased rapidly and linearly afterward. The bolus aspect ratio $a/L = 0.4 \pm 0.1$, and by extension the bolus Iribarren number $\xi_b = 0.08 \pm 0.01$, remained constant throughout the up-slope evolution.

[14] Figure 5 shows the time series of the acoustic backscatter and anomaly currents induced by the passage of the wavetrain over Moorings B and C. The observations at Mooring B are similar to those at Mooring A (not shown) and revealed that the wavetrain was composed of 3 large waves (6 m $< a <$ 8 m) of period $T \simeq 200$ s followed by 12 smaller amplitude waves (2 m $< a <$ 4 m). A close inspection of Figure 5 reveals that, by the time the wavetrain reached Mooring C, 270 m further upslope, it had disintegrated into 18 ± 1 boluses. These boluses are characterized as irregularly spaced, near-bottom and short-duration signals of the density (superimposed on a longer timescale depression of the pycnocline), backscatter intensity and currents. The bolus-induced density fluctuations of around 2 kg m^{-3} indicate that they transport dense water upslope. This upslope transport of dense water by the boluses is also seen in the numerical results. The timescale of the wavetrain shoaling event $T_m \simeq 5000$ s is taken as the period between the time the leading wave entered the slope region ($t = 0$) and the time the last bolus went over Mooring C.

4. Energetics, Reflectance, and Mixing

[15] The energy, per unit of crest length, of the three leading solitary-like waves impacting the slope was estimated to be $E_0 = 230 \pm 40$ kJ m^{-1}. This value was inferred by combining velocity data from the ADCP at Mooring A with a normal mode structure of the waves using the density profile shown on Figure 3. The energy E_0' of the smaller amplitude trailing waves was more difficult to determine, given their complex signal. An order of magnitude calculation based on two-layer linear wave theory [*Kundu*, 1990] gave $E_0' \sim 100$ kJ m^{-1}.

[16] The fraction of E_0 that reflected at impact was estimated using the *Bourgault and Kelley* [2007] parametrization for the reflectance R of uniform slopes for normally incident ISWs, i.e. $R = 1 - e^{-\xi/\xi 0}$, with $\xi_0 = 0.78 \pm 0.02$. Using $\xi = 0.16$ gives $R = 0.19$. The reflected portion of the incoming wavetrain could not be unambiguously extracted from the mooring observations but is clearly seen in the numerical simulations for the case of a single impinging ISW (Figure 2).

[17] From his laboratory experiments on shoaling ISWs, *Helfrich* [1992] found that a fraction $\Gamma = 0.15 \pm 0.05$ of the unreflected wave energy is lost to irreversible turbulent mixing in the slope region during the shoaling process, independently of the Iribarren number ξ. In a similar experiment, *Michallet and Ivey* [1999] found a dependance of Γ on ξ: for $\xi = 0.2$ (i.e. their lowest value examined) they

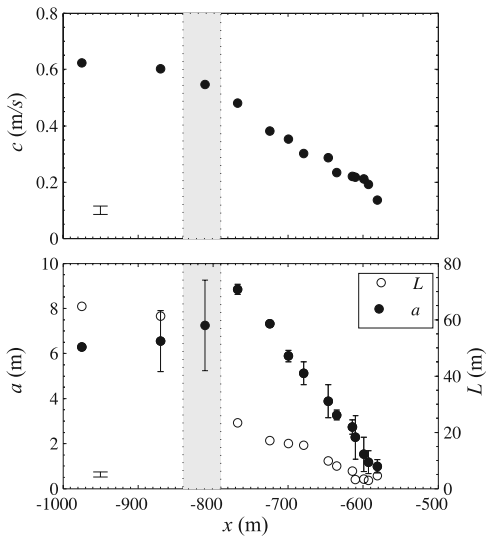

Figure 4. (top) The leading wave phase speed c, (bottom) amplitude a and wavelength L as a function of distance from the island. The grey boxes represent the region over which the transition from a wave of depression to a wave of elevation (or bolus) occurred. Errorbars for c and L are shown at the lower left corner of the corresponding panels. The lengthscale was not measured during the transition phase.

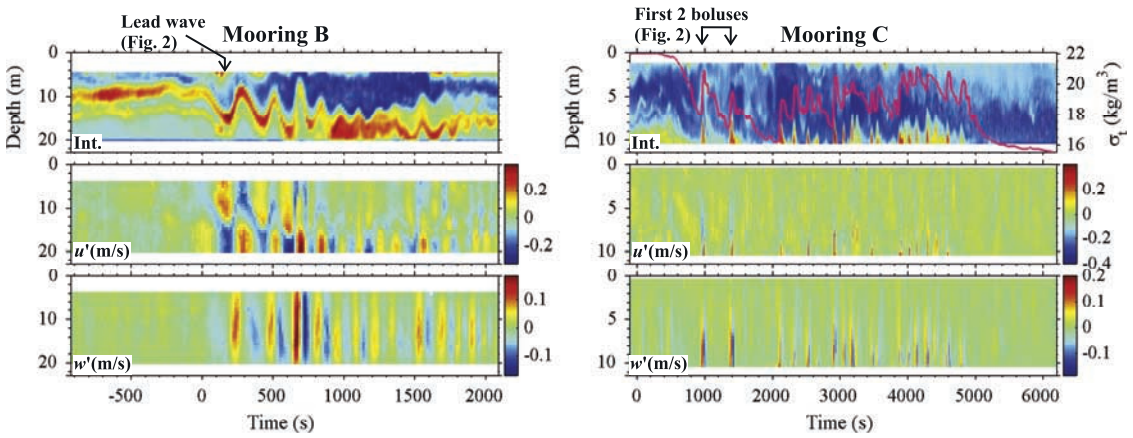

Figure 5. Acoustic backscatter intensity (in relative units), horizontal u' and vertical w' (positive up) wave-induced currents at Moorings (left) B and (right) C. The prime indicates that the variables have been highpass filtered using a fourth-order Butterworth filter with a cutoff frequency of 10^{-3} Hz. Also shown is the near-bottom density anomaly σ_t at Mooring C (magenta curve). Time is relative to the first panel of Figure 2.

found $\Gamma = 0.07 \pm 0.01$ (see *Boegman et al.* [2005] for a re-interpretation of the *Michallet and Ivey* [1999] measurements in terms of ξ). Applying these results to our field site suggests that the impact of the 3 leading waves on the slope increased the mean potential energy of the system by $\Delta P = \Gamma E_0 (1-R) = 27 \pm 17$ kJ m^{-1}. Assuming that the mixing took place over the length L_m and over the timescale T_m yields a buoyancy flux per unit area $J = \Delta P/(T_m L_m) = 0.023 \pm 0.015$ W m^{-2}. We did not attempt to quantify the mixing caused by the trailing waves, so the above estimate of the wavetrain-induced buoyancy flux should be considered a conservative lower bound.

5. Discussion and Conclusion

[18] Our field measurements are in good agreement with the laboratory measurements of *Helfrich* [1992] for ISW run-up on uniform slopes. A fit to his measurements (shown in Helfrich's Figure 12) shows that the amplitude decay rate of the laboratory leading bolus is linear with $(L_m/a_0)\partial a/\partial x = -1.1$, where a_0 is the initial bolus amplitude and L_m is the distance over which the bolus decays. Our field measurements also display a linear decay rate for the amplitude of the leading bolus (Figure 4) with $(L_m/a_0)\ \partial a/\partial x = -1.1 \pm 0.1$. We found that the aspect ratio of the bolus had a constant value, $a/L = 0.4 \pm 0.1$, throughout the run-up process. This is consistent with the laboratory findings of *Helfrich* [1992] of constant bolus aspect ratio $a/L_b = 0.3 \pm 0.1$, independent of bottom slope. Here, L_b is the length of the base of the bolus; expressed in the same way, we measured $a/L_b = 0.28 \pm 0.02$ in the St. Lawrence Estuary.

[19] In their respective field studies, *Klymak and Moum* [2003] and *Scotti and Pineda* [2004] raised a number of hypotheses and questions regarding the origin and evolution of shoaling ISWs of elevation, similar to our boluses, in coastal environments.

[20] *Klymak and Moum* [2003] hypothesized, by analogy to breaking surface waves on beaches, that the ISWs of elevation they observed on the Oregon Shelf might have later ended abruptly further upshelf. This is a process we did not observe. Given the self-preserving nature of the shape of a bolus shoaling on a uniform slope, we hypothesize that those waves observed by *Klymak and Moum* [2003] did not end abruptly but rather decayed gradually as in the present study. The same reasoning can be applied to the waves observed in Massachusetts Bay by *Scotti and Pineda* [2004].

[21] Both of those studies considered that a fundamental question is how far such features can propagate inshore. The detailed echosounding and moored observations in the St Lawrence Estuary described in this paper provide an answer in one case (Figure 2). The good qualitative agreement between the field observations and the two-dimensional nonhydrostatic numerical simulations presented here encourages the use of numerical models for predicting the evolution of shoaling ISWs in regions where field observations are less detailed.

[22] Returning to the issue of parameterization, *Klymak and Moum* [2003] questioned the origin of the waves of elevation. Our field observations show one mechanism by which boluses or waves of elevation can be generated from shoaling waves of depression. This process was hypothesized by *Scotti and Pineda* [2004] and has been observed in the South China Sea [*Orr and Mignerey*, 2003]. In order to make progress in developing a parameterization of ISW-induced mixing, it will be necessary to identify the source of the original ISWs of depression. In our case these are presumably tidally-driven [*Bourgault and Kelley*, 2003; *Bourgault et al.*, 2005] but their exact origin and generation mechanism remain to be determined.

[23] **Acknowledgments.** We would like to thank our collaborators Alex Hay, Peter Galbraith, and Brad deYoung for their contribution to the scientific planning, logistics and participation to the field work. We thank Jack Foley, Daniel Thibault, Rémi Desmarais, Douglas Schillinger and the captain and crew of the CCGC Isle Rouge for the instrument preparation, deployment and recovery. We are also thankful to the anonymous reviewers for their constructive comments. This work was supported by the Canadian Foundation for Climate and Atmospheric Sciences, the Natural Sciences and Engineering Research Council of Canada and the Department of Fisheries and Oceans of Canada.

References

Boegman, L., G. N. Ivey, and J. Imberger (2005), The degeneration of internal waves in lakes with sloping topography, *Limnol. Oceanogr.*, *50*, 1620–1637.

Bourgault, D., and D. E. Kelley (2003), Wave-induced boundary mixing in a partially mixed estuary, *J. Mar. Res.*, *61*(5), 553–576.

Bourgault, D., and D. E. Kelley (2007), On the reflectance of uniform slopes for normally incident interfacial solitary waves, *J. Phys. Oceanogr.*, in press.

Bourgault, D., D. E. Kelley, and P. S. Galbraith (2005), Interfacial solitary wave run-up in the St. Lawrence Estuary, *J. Mar. Res.*, *63*(6), 1001–1015.

Helfrich, K. R. (1992), Internal solitary wave breaking and run-up on a uniform slope, *J. Fluid Mech.*, *243*, 133–154.

Helfrich, K. R., and W. K. Melville (2006), Long nonlinear internal waves, *Annu. Rev. Fluid Mech.*, *38*, 395–425.

Klymak, J. M., and J. N. Moum (2003), Internal solitary waves of elevation advancing on a shoaling shelf, *Geophys. Res. Lett.*, *30*(20), 2045, doi:10.1029/2003GL017706.

Kundu, P. K. (1990), *Fluid Mechanics*, Elsevier, New York.

Michallet, H., and G. N. Ivey (1999), Experiments on mixing due to internal solitary waves breaking on uniform slopes, *J. Geophys. Res.*, *104*(C6), 13,467–13,477.

Orr, M. H., and P. C. Mignerey (2003), Nonlinear internal waves in the South China Sea: Observation of the conversion of depression internal waves to elevation internal waves, *J. Geophys. Res.*, *108*(C3), 3064, doi:10.1029/2001JC001163.

Scotti, A., and J. Pineda (2004), Observation of very large and steep internal waves of elevation near the Massachusetts coast, *Geophys. Res. Lett.*, *31*, L22307, doi:10.1029/2004GL021052.

Venayagamoorthy, S. K., and O. B. Fringer (2006), Numerical simulations of the interaction of internal waves with a shelf break, *Phys. Fluids*, *18*, 076603.

Venayagamoorthy, S. K., and O. B. Fringer (2007), On the formation and propagation of nonlinear internal boluses across a shelf break, *J. Fluid Mech.*, in press.

M. D. Blokhina and D. Bourgault, Department of Physics and Physical Oceanography, Memorial University of Newfoundland, St. John's, NL, Canada A1B 3X7. (marina@physics.mun.ca; danielb@physics.mun.ca)

D. Kelley and R. Mirshak, Department of Oceanography, Dalhousie University, 1355 Oxford Street Halifax, NS, Canada B3H 4J1. (dan.kelley@dal.ca; ramzi@dal.ca)